

Numerical simulation of injectivity loss in stratified reservoirs

J. S. Wrobel^{1,*}, A. Nachbin², D. Marchesin²

¹ *Departamento de Matemática, Universidade Federal do Espírito Santo (UFES)
Avenida Fernando Ferrari, 514, 29075-910, Vitória - ES - Brazil*

² *Instituto Nacional de Matemática Pura e Aplicada (IMPA)
Estrada Dona Castorina, 110, 22460-320, Rio de Janeiro - RJ - Brazil*

SUMMARY

Injectivity loss occurs when sea water is injected in offshore fields or during reinjection of produced water that contains solid particles, oil drops and bacteria, each one with its own capability of reducing the permeability in the neighborhood of the well. Knowledge regarding the causes of injectivity decline and its time scale is important for the prevention and remediation of this problem. We present a numerical model for water injection with retention of solid particles in a vertically stratified reservoir in a cylindrical axisymmetric geometry. The process of migration and retention of solid particles in porous media is studied through computer simulations. To do so, we apply a hydrodynamical formulation for the flow of water containing suspension particles. The numerical tools used in this work are the modified method of characteristics proposed by Douglas and Russell for the concentration of particles (suspended and retained) coupled with the mixed finite element method proposed by Raviart and Thomas for velocity and pressure. We briefly describe the method and show the numerical results. There is a strong tendency for the flow to remain confined in each layer. Copyright © 2000 John Wiley & Sons, Ltd.

KEY WORDS: injectivity loss; porous media; finite element method; method of characteristics

1. INTRODUCTION

In oil recovery, usually water is injected in some wells, while oil and water are produced at others. The injection of water containing organic and inorganic particles in suspension causes retention of these particles in the neighborhood of the well. Consequently reduction of permeability is observed and the well can become useless. On the other hand, removing these particles before injection is an expensive process that consumes a considerable amount of energy and requires large equipment, which is critical in offshore exploitation. So, the study of injectivity loss is of great importance for offshore oil recovery to maintain rates of injection and therefore the oil production.

*Correspondence to: Departamento de Matemática, Universidade Federal do Espírito Santo (UFES)
Avenida Fernando Ferrari, 514, 29075-910, Vitória - ES - Brazil

Mathematical models for this phenomenon constitute an important tool to understand mechanisms for permeability loss. The knowledge of conditions that cause injectivity loss, when and where it occurs, help in the prevention and correction of problems of this nature.

In this context, this work discusses damage formation due to deep filtration during injection of water containing solid particles. The new feature is that we take into account the rock strata. A numerical model for water injection with retention of particles is developed in a vertically stratified reservoir for 3D-axisymmetric flows, coupling the mixed finite elements method for pressure and velocity with a modified method of characteristics for the water and particle motion and retention. We study the effect of particle retention in the presence of a stratified subsurface.

2. MATHEMATICAL MODEL

Consider a flow of water with suspended particles entering in a vertically stratified porous medium, as shown in figure 1. As time evolves, the suspended particles are retained in the pores, reducing the permeability of this medium. The porosity ϕ remains constant.

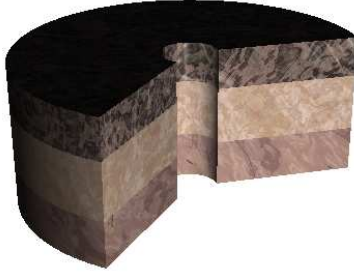


Figure 1. Neighborhood of the well, in an stratified porous media.

According with [7], diffusion can be neglected for particles larger than $1 \mu m$ and it has little importance for small particles. Having this in mind and considering incompressible flow, the mass conservation equation for suspended (\tilde{c}) and retained ($\tilde{\sigma}$) particles, if particle density is equal to water density, can be written as

$$\frac{\partial}{\partial t}(\phi\tilde{c} + \tilde{\sigma}) + \tilde{\mathbf{u}} \cdot \nabla\tilde{c} = 0, \quad (1)$$

where $\tilde{\mathbf{u}}$ is the flow velocity, and the incompressibility of the suspension is written as

$$\nabla \cdot \tilde{\mathbf{u}} = 0. \quad (2)$$

Permeability is a decreasing function of retained concentration. So, Darcy's law relating flow velocity ($\tilde{\mathbf{u}}$) and pressure gradient (p) becomes

$$\tilde{\mathbf{u}} = -\frac{K}{\mu}k(\tilde{\sigma})\nabla\tilde{p} \quad (3)$$

where μ is the viscosity of the fluid, K is the absolute permeability of the porous medium and $k(\tilde{\sigma})$ is called the formation damage function. In general, viscosity depends on the concentration

of the particles but we will neglect this effect for small concentrations. Prediction of the formation damage function is a problem of choosing a model expressing $k(\sigma)$ in accordance with other properties of the rock.

The particle retention rate is

$$\frac{\partial \tilde{\sigma}}{\partial t} \propto \tilde{\lambda}(\tilde{c}, \tilde{\sigma}, \tilde{\mathbf{u}}). \quad (4)$$

A specific form for $\tilde{\lambda}$ will be given below. This formula tells us that the probability of retention of particles in the medium depends on the velocity of the fluid as well as on the concentration of suspended and retained particles. See the proportionality relation proposed below.

System (1)-(4) gives the evolution of the velocity ($\tilde{\mathbf{u}}$), pressure (\tilde{p}) and concentration of suspended (\tilde{c}) and retained ($\tilde{\sigma}$) particles.

We are considering an axisymmetric geometry so our system is written in cylindrical coordinates. Because of that, the operators ∇ and $\nabla \cdot$ mean

$$\begin{aligned} \nabla \tilde{p} &= \left(\frac{\partial \tilde{p}}{\partial \tilde{r}}, \frac{\partial \tilde{p}}{\partial \tilde{z}} \right), \\ \nabla \cdot \tilde{\mathbf{u}} &= \left(\frac{1}{\tilde{r}} \frac{\partial}{\partial \tilde{r}} (\tilde{r} \tilde{u}) + \frac{\partial \tilde{v}}{\partial \tilde{z}} \right). \end{aligned}$$

2.1. Empirical Functions

In this work, we will follow the works of [2], [3], [8], [11] and consider loss of permeability as a function of retained particle density given by

$$k(\tilde{\sigma}) = (1 + \beta \tilde{\sigma})^{-1}, \quad (5)$$

where β is the damage coefficient, an empirical parameter related to change in tortuosity when particles are retained in the pores.

The particle retention rate is written in the form proposed in [7], which is valid if $\tilde{\sigma} \ll \phi$:

$$\frac{\partial \tilde{\sigma}}{\partial t} = \tilde{\lambda}(\tilde{\sigma}) |\tilde{\mathbf{u}}| \tilde{c}. \quad (6)$$

The proportionality coefficient $\tilde{\lambda}$, called the filtration coefficient, is a function of the retained particle density $\tilde{\sigma}$. This function depends on the geometry of the porous space and on the mineral content of the rock surface and it should be determined from laboratory coreflood tests.

In the numerical method presented here more general functions can be used without any difficulty.

2.2. Nondimensionalization

Using the characteristic scales we define dimensionless variables (without tildes)

$$r_0 = \tilde{r}_0, \quad (7a)$$

$$r = \frac{1}{r_0} \tilde{r}, \quad z = \frac{1}{r_0} \tilde{z}, \quad t = \frac{1}{T} \tilde{t}, \quad (7b)$$

$$u = \frac{T}{r_0} \tilde{u}, \quad v = \frac{T}{r_0} \tilde{v}, \quad (7c)$$

$$c = \tilde{c}, \quad \sigma = \tilde{\sigma}, \quad (7d)$$

$$\lambda = r_0 \tilde{\lambda}, \quad (7e)$$

$$p = \frac{\overline{K} T}{\mu r_0^2} \tilde{p}, \quad \overline{K} = \frac{1}{2\pi H((\tilde{r}_0 + L)^2 - \tilde{r}_0^2)} \int_0^H \int_{\tilde{r}_0}^{\tilde{r}_0 + L} \tilde{K}(\tilde{r}, \tilde{z}) \tilde{r} d\tilde{r} d\tilde{z}. \quad (7f)$$

where r_0 is the radius of the well, T is the typical time until a particle is captured by a pore and L is a typical filtration distance. Also u and v are respectively the horizontal and vertical components of the velocity \mathbf{u} . The parameter \overline{K} represents an average over the formation height H .

Substituting this scaling in (1), (2), (3), (6), our final system takes the form

$$\phi \frac{\partial c}{\partial t} + \mathbf{u} \cdot \nabla c = -\lambda(\sigma) c |\mathbf{u}|, \quad (8)$$

$$\frac{\partial \sigma}{\partial t} = \lambda(\sigma) c |\mathbf{u}|, \quad (9)$$

$$\mathbf{u} = -\frac{K}{\overline{K}} k(\sigma) \nabla p, \quad (10)$$

$$\nabla \cdot \mathbf{u} = 0. \quad (11)$$

2.3. Initial and Boundary Conditions

It is necessary to establish initial and boundary conditions for system (8) - (11). The initial condition is the absence of particles in the medium before the injection

$$c(r, 0) = 0 \quad \text{and} \quad \sigma(r, 0) = 0 \quad \text{at} \quad t = 0. \quad (12)$$

The boundary conditions correspond to fluid injection at the well, with prescribed suspended particle concentration and flow rate, and zero vertical velocity at the top and the bottom of the domain (that is, the rock is impermeable at these boundaries):

$$c(r_0, z, t) = c_i \quad \text{and} \quad (13)$$

$$q(r_0, z, t) = q_i \quad (14)$$

$$v = 0 \quad \text{at} \quad z = 0 \quad (15)$$

$$v = 0 \quad \text{at} \quad z = H/r_0 \quad (16)$$

where c_i and q_i are positive constants. We get the boundary condition for σ from equation (9).

2.4. Overview of the Numerical Method

To solve the system we couple two numerical methods. First we write discrete equations for pressure and velocity using mixed finite elements, specifically, lowest order Raviart-Thomas [9]. This method is very useful in our model because we can solve pressure and velocity together and we do not need to take a numerical pressure gradient to find the velocity. Another advantage is that we get a linear system with a symmetric positive definite (*spd*) matrix, so we can use a conjugate gradient method to solve it. Once we know the velocity, we can advance the equations for suspended and retained particles by one time step. To do that, we use the method of characteristics [6] in both equations. The method of characteristics is very stable and we do not need to use very small time steps. **It is simple, computationally economic and we have a large experience in such method. For this particular problem, we controled total mass and we do not observed a significative loss of mass. Nevertheless the use of conservative methods like [5] and [10] in the future are not discarded.**

3. NUMERICAL METHOD

The numerical method to solve (8)-(15) is divided into two blocks. First, we solve the equations for velocity and pressure using the mixed finite element method. Then, with the updated velocity, we use the method of characteristics to advance in time the equations for the suspended and retained particles. We will describe each step.

3.1. Mixed Finite Element Method

For the first part of the method we focus on

$$\nabla \cdot \mathbf{u} = 0 \quad (17)$$

$$\mathbf{u} = -\alpha(\sigma)\nabla p \quad (18)$$

on the domain $\Omega = [1, 1 + L/r_0] \times [0, H/r_0]$, where $\alpha(\sigma) = Kk(\sigma)/\overline{K}$. To solve this part of the system, we follow [9], [12]. Multiplying equation (18) by α^{-1} and integrating with a test function \mathbf{v} , we get

$$\int_{\Omega} \alpha^{-1} \mathbf{u} \cdot \mathbf{v} \, d\Omega + \int_{\Omega} \nabla p \cdot \mathbf{v} \, d\Omega = 0, \quad \forall \mathbf{v} \in H(\text{div}, \Omega), \quad (19)$$

where $H(\text{div}, \Omega) := \{\boldsymbol{\tau} \in L^2(\Omega) | \nabla \cdot \boldsymbol{\tau} \in L^2(\Omega)\}$ [4]. Using the Divergence Theorem,

$$\int_{\Omega} \alpha^{-1} \mathbf{u} \cdot \mathbf{v} \, d\Omega - \int_{\Omega} p \nabla \cdot \mathbf{v} \, d\Omega = - \int_{\partial\Omega} p \mathbf{v} \cdot \mathbf{n} \, ds \quad (20)$$

$\forall \mathbf{v} \in H(\text{div}, \Omega)$. Equation (17) can also be integrated with a test function q to obtain

$$\int_{\Omega} \nabla \cdot \mathbf{u} q \, d\Omega = 0, \quad \forall q \in L^2(\Omega).$$

So, the variational problem related to system (17), (18) is to find $(\mathbf{u}, p) \in (H(\text{div}, \Omega), L^2(\Omega))$ such that

$$\int_{\Omega} \alpha^{-1} \mathbf{u} \cdot \mathbf{v} \, d\Omega - \int_{\Omega} p \nabla \cdot \mathbf{v} \, d\Omega = - \int_{\partial\Omega} p \mathbf{v} \cdot \mathbf{n} \, ds, \quad (21)$$

$$\int_{\Omega} \nabla \cdot \mathbf{u} q \, d\Omega = 0, \quad (22)$$

$\forall \mathbf{v} \in H(\text{div}, \Omega), \forall q \in L^2(\Omega)$.

Considering $r_i = r_0 + i\Delta r$ e $z_i = z_0 + i\Delta z$, with $i \in \mathbb{Z}^+$ for each element E of our discretization, we have the subspaces $V_h(E)$ e $Q_h(E)$ given by their respective bases:

$$V_h(E) = \left\{ \begin{array}{l} \xi_1 = \begin{pmatrix} 1 - (r - r_i)/\Delta r \\ 0 \\ 0 \end{pmatrix}, \quad \xi_2 = \begin{pmatrix} (r - r_i)/\Delta r \\ 0 \\ 0 \end{pmatrix}, \\ \xi_3 = \begin{pmatrix} 0 \\ 0 \\ 1 - (z - z_i)/\Delta z \end{pmatrix}, \quad \xi_4 = \begin{pmatrix} 0 \\ 0 \\ (z - z_i)/\Delta z \end{pmatrix}. \end{array} \right.$$

$$Q_h(E) = \psi = \begin{cases} 1 & \text{in } E, \\ 0 & \text{out of } E. \end{cases}$$

The functions \mathbf{u}_h and p_h we are looking for can be written as a linear combination of basis elements. Within a given finite element the four global indices are identified with local indices as for example $k_a \Leftrightarrow 1, k_b \Leftrightarrow 2, k_c \Leftrightarrow 3, k_d \Leftrightarrow 4$, where k_a, \dots, k_d are the global indices running from 1 to $(m+1)n$ in the horizontal coordinate and $m(n+1)$ in the vertical one. With this dual notation one easily has the corresponding local basis functions (the polynomials ξ in r and z).

$$\mathbf{u}_h(r, z) = \left(\sum_{k=1}^{(m+1)n} u_k \xi_k(r, z), \sum_{k=1}^{m(n+1)} v_k \xi_k(r, z) \right) \quad (23)$$

$$p_h(r, z) = \sum_{k=1}^{mn} p_k \psi_k(r, z). \quad (24)$$

It is important to notice that, since the normal component of \mathbf{u} is constant on the faces of the elements, we can construct a vector space of finite dimension in Ω with continuous normal component at the interface of two elements that are in a subspace of $H(\text{div}, \Omega)$, where the velocity is defined.

The mixed finite element problem is to find $(\mathbf{u}_h, p_h) \in V_h \times Q_h$ such that

$$\int_{\Omega} \alpha^{-1} \mathbf{u}_h \mathbf{v}_h \, d\Omega - \int_{\Omega} p_h \nabla \cdot \mathbf{v}_h \, d\Omega = - \int_{\partial\Omega} p_h \mathbf{v}_h \cdot \mathbf{n} \, ds \quad (25)$$

$$\int_{\Omega} q_h \nabla \cdot \mathbf{u}_h \, d\Omega = 0 \quad (26)$$

$\forall \mathbf{v}_h \in V_h(\Omega), \forall q_h \in Q_h(\Omega)$.

Utilizing the expressions (23) and (24) for \mathbf{u}_h e p_h , our discretized system (25)-(26) takes the form

$$\begin{aligned} A\mathbf{u}_h + B^T p_h &= f \\ B\mathbf{u}_h &= 0. \end{aligned}$$

We used Usawa accelerator [4] to solve our system. First, we eliminate \mathbf{u} and then we solve the system in p . From the first equation,

$$\mathbf{u} = A^{-1}(f - B^T p).$$

Substituting in the second equation, we get

$$BA^{-1}B^T p = BA^{-1}f,$$

or, in a simplified form

$$Cp = d, \tag{27}$$

with $C = BA^{-1}B^T$ and $d = BA^{-1}f$. The matrix A is tridiagonal and easily invertible and we can show that the matrix C is symmetric positive definite (*spd*). To solve the new system (27), we will use the conjugate gradient method. This method is extremely efficient to solve systems with *spd* sparse matrices because at each iteration we just need to store a small number of vectors.

Since we know \mathbf{u} we can put it in equations (8) and (9) to solve for c and σ , namely to advance them by one time step. To do so, we will use the method of characteristics, shown in next subsection.

3.2. Method of Characteristics

In each of the procedures to be treated below, we shall consider a time step $\Delta t > 0$ and approximate solutions at times $t^n = n\Delta t$.

Considering the velocity given at time t^{n-1} , we want to solve equations (8) and (9), namely

$$\phi \frac{\partial c}{\partial t} + \mathbf{u} \cdot \nabla c = -\lambda(\sigma)c|\mathbf{u}| \tag{28}$$

$$\frac{\partial \sigma}{\partial t} = \lambda(\sigma)c|\mathbf{u}|, \tag{29}$$

in order to calculate c e σ at time t^n . We will use the method of characteristics that we will describe following [6], [12].

Defining

$$\psi(\mathbf{x}) = \sqrt{\phi^2 + |\mathbf{u}(\mathbf{x})|^2}, \tag{30}$$

the differentiation in the characteristic direction $\tau = \tau(\mathbf{x})$, associated with the operator $\phi c_t + \mathbf{u} \cdot \nabla c$, is given by

$$\frac{\partial}{\partial \tau(\mathbf{x})} = \frac{1}{\psi(\mathbf{x})} \left(\phi \frac{\partial}{\partial t} + \mathbf{u} \cdot \nabla \right). \tag{31}$$

Then, the left side of equation (28) can be put in the form

$$\phi \frac{\partial c}{\partial t} + \mathbf{u} \cdot \nabla c = \psi \frac{\partial c}{\partial \tau}. \quad (32)$$

The characteristic derivative will be approximated basically in the following manner: consider a mesh point \mathbf{x} at time t^n . Follow the characteristic related to the derivative $\partial/\partial\tau$ that passes through (\mathbf{x}, t^n) , back to the location $(\bar{\mathbf{x}}, t^{n-1})$. Denote this departure point by $\bar{\mathbf{x}}$:

$$\bar{\mathbf{x}} = \mathbf{x} - \frac{\mathbf{u}(\mathbf{x}, t^n)}{\phi} \Delta t. \quad (33)$$

Notice that

$$\psi \frac{\partial u}{\partial \tau} \approx \psi(\mathbf{x}) \frac{u(\mathbf{x}, t^n) - u(\bar{\mathbf{x}}, t^{n-1})}{\Delta \tau}.$$

But $(\Delta \tau)^2 = (\mathbf{x} - \bar{\mathbf{x}})^2 + (\Delta t)^2$, so

$$\psi \frac{\partial u}{\partial \tau} \approx \psi(\mathbf{x}) \frac{u(\mathbf{x}, t^n) - u(\bar{\mathbf{x}}, t^{n-1})}{[(\mathbf{x} - \bar{\mathbf{x}})^2 + (\Delta t)^2]^{1/2}}. \quad (34)$$

Substituting equation (30) and (33) in (34), we have

$$\psi \frac{\partial u}{\partial \tau} \approx c(\mathbf{x}) \frac{u(\mathbf{x}, t^n) - u(\bar{\mathbf{x}}, t^{n-1})}{\Delta t}.$$

The discretization of the left hand side of equation (28) considering $c_i^n = c(\mathbf{x}_i, t^n)$ and $\bar{c}_i^{n-1} = c(\bar{\mathbf{x}}, t^{n-1})$ is given by

$$\phi \frac{\partial c}{\partial t} + \mathbf{u} \cdot \nabla c \approx \phi \frac{c_i^n - \bar{c}_i^{n-1}}{\Delta t}.$$

The right hand side of equation (28) is approximated by the average between times t^{n-1} and t^n , since we are considering a centered difference at time $t^{n+1/2}$, namely

$$\phi \frac{c_i^n - \bar{c}_i^{n-1}}{\Delta t} = \frac{1}{2} \{ \lambda(\sigma_i^n) c_i^n |\mathbf{u}_i^n| + \lambda(\bar{\sigma}_i^{n-1}) \bar{c}_i^{n-1} |\bar{\mathbf{u}}_i^{n-1}| \}.$$

We can rewrite this evolution step in a more appropriate fashion:

$$c_i^n = \frac{\phi - (\Delta t/2) \lambda(\bar{\sigma}_i^{n-1}) |\bar{\mathbf{u}}_i^{n-1}|}{\phi + (\Delta t/2) \lambda(\sigma_i^n) |\mathbf{u}_i^n|} \bar{c}_i^{n-1}. \quad (35)$$

Now, consider equation (29). The characteristics here are vertical and to go back in time following characteristic lines is exactly the same as using finite differences. So, this equation takes the discretized form

$$\frac{\partial \sigma}{\partial t} \approx \frac{\sigma_i^n - \sigma_i^{n-1}}{\Delta t}.$$

Taking again an average for the right hand side and rearranging, we get

$$\sigma_i^n = \sigma_i^{n-1} + \frac{\Delta t}{2} (\lambda(\sigma_i^n) c_i^n |\mathbf{u}_i^n| + \lambda(\sigma_i^{n-1}) c_i^{n-1} |\mathbf{u}_i^{n-1}|). \quad (36)$$

Now, we can substitute equation (35) in (36) to obtain an implicit formula in σ :

$$\sigma_i^n = \sigma_i^{n-1} + \frac{\Delta t}{2} \left(\lambda(\sigma_i^n) \frac{\phi - (\Delta t/2)\lambda(\bar{\sigma}_i^{n-1})|\bar{\mathbf{u}}_i^{n-1}|}{\phi + (\Delta t/2)\lambda(\sigma_i^n)|\mathbf{u}_i^n|} \bar{c}_i^{n-1} |\mathbf{u}_i^n| + \lambda(\sigma_i^{n-1}) c_i^{n-1} |\mathbf{u}_i^{n-1}| \right). \quad (37)$$

Once we know the values of σ , we can substitute them in equation (35) to update the values of c . To do that, we procede as follows:

Let $c_h(\mathbf{x}, t^n)$, $\sigma_h(\mathbf{x}, t^n)$ be the approximate solutions of (28), (29). Formula (37) tells us that to calculate the approximate solution at time t^n we only need to know the solution at points (\mathbf{x}, t^{n-1}) and $(\bar{\mathbf{x}}, t^{n-1})$. The problem is that usually the latter points are not mesh points. So, to calculate the solutions $c_h(\mathbf{x}, t^n)$, $\sigma_h(\mathbf{x}, t^n)$ we need to interpolate values $u_h(\mathbf{x}_i, t^{n-1})$ using the known values at the neighboring mesh points. To interpolate these points we will use cubic Lagrange interpolation in the following manner (figure 2a): assume that we want to interpolate a point at position X . We will use the horizontal component of this point and we will perform a cubic Lagrange interpolation at each of the four horizontal lines, using the points marked with a white ball. In this way, we can find interpolated values at black balls. Now, we can perform a vertical cubic Lagrange interpolation using these black ball values in order to determine the value at X . To interpolate points in boundary elements, we can use a bilinear interpolation or we can shift the points used in the interpolation (figure 2b). We chose the second option. This kind of interpolation is successfully used in Numerical Weather Prediction and has a computational advantage of requiring just one calculation for the horizontal weights for each interpolated point.

Since we know the solution at time t^{n-1} in the mesh points (\mathbf{x}, t^{n-1}) we can calculate $(\bar{\mathbf{x}}, t^{n-1})$ using the numerical interpolation method described above. Then we use equation (37) to update σ in time, that is, to find the values of $\sigma(\mathbf{x}, t^n)$ using Newton's Method, since this equation is nonlinear. With these values of $\sigma(\mathbf{x}, t^n)$ we use equation (35) to update c , that is, to find $c(\mathbf{x}, t^n)$.

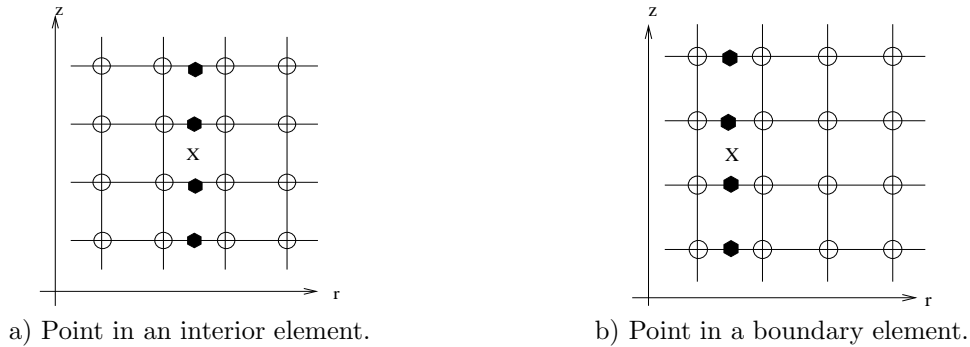


Figure 2. Interpolation scheme used in the characteristic method.

4. ANALYTICAL AND NUMERICAL BOUNDARY CONDITION

In our numerical scheme, we considered pressure given as a boundary condition. But in the real world, for the petroleum industry, the significant parameter is the injection flow rate.

There is a tendency to maintain constant injection flow rate to guarantee a regular production of oil. Therefore we adjust our model so that we can specify the total flow rate as a boundary condition, as shown in picture 3.

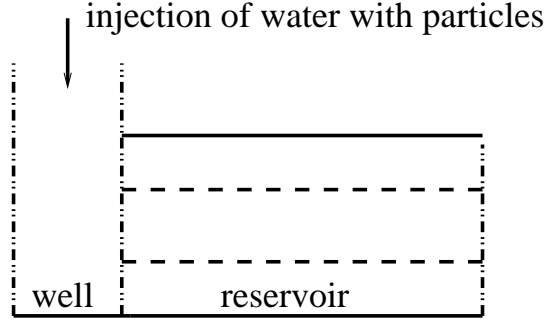


Figure 3. Injection of particles in the reservoir.

To use the method as described above we have to be careful with the boundaries. The difficulty is that knowing the injection flow rate is insufficient for solving the problem since we do not know how it is distributed vertically. Once the flow rate is given and the deposition mechanism begins, we have to adjust the pressure at each time step to maintain the specified total flow rate.

Consider the neighborhood of the well (on a more general setup than we considered before) with properties that change both in the horizontal and vertical directions. The horizontal component of equation (10) is

$$u(r, z) = -\frac{K_1(r, z)}{\bar{K}} k_1(\sigma(r, z)) \frac{\partial p(r, z)}{\partial r}.$$

Here, $u(r, z)$, $\sigma(r, z)$, $p(r, z)$, $K_1(r, z)$ and $k_1(\sigma(r, z))$ mean respectively horizontal velocity, concentration of retained particles, pressure and the horizontal component of K and k at time t^{n-1} . Rearranging and integrating in r , we get that the pressure differential is Δp :

$$\bar{K} \int_1^{1+L/r_0} \frac{u(r, z)}{K_1(r, z)k_1(\sigma(r, z))} dr = \int_1^{1+L/r_0} -\frac{\partial p(r, z)}{\partial r} dr = p(1, z) - p(1 + L/r_0, z) = \Delta p.$$

Integrating in z and dividing by H , it becomes

$$\Delta p = \frac{\bar{K}}{H} \int_0^H \int_1^{1+L/r_0} \frac{u(r, z)}{K_1(r, z)k_1(\sigma(r, z))} dr dz. \quad (38)$$

At the inlet, the flow rate through an infinitesimal layer dz is given by

$$dQ = u(1, z)2\pi dz.$$

Integrating in z , the total flow rate at the inlet is

$$Q = 2\pi \int_0^H u(1, z) dz. \quad (39)$$

Equations (38) and (39) allow us to adjust the pressure boundary conditions at each time step for an anisotropic medium.

The calculation of the pressure as a function of flow rate is not straightforward but we will see that it simplifies a lot for a layered medium.

Let us use the calculation above for the case of a medium with non-communicating horizontal layers, meaning that there is no flow between layers. In each layer j , the horizontal component of equation (10) is

$$u^j(r) = -\frac{K^j}{\bar{K}} k(\sigma^j) \frac{\partial p^j}{\partial r}. \quad (40)$$

If the flow rate in each layer is denoted by q^j , then

$$u^j(r) = \frac{q^j}{2\pi r h^j}, \quad (41)$$

where h^j is the height of layer j and the vertical component v will be zero. Substituting (41) in (40) and integrating in r , we obtain

$$\Delta p^j = \frac{q^j}{2\pi h^j} \frac{\bar{K}}{K^j} \int_1^{1+L/r_0} \frac{1}{rk(\sigma^j)} dr,$$

with $\Delta p^j = p^j(1) - p^j(1 + L/r_0)$. But $\Delta p^j = \Delta p$. So, this equation tells us that the flow rate in each layer is given by

$$q^j = 2\pi h^j \frac{K^j}{\bar{K}} \left(\int_1^{1+L/r_0} \frac{dr}{rk(\sigma^j)} \right)^{-1} \Delta p.$$

Since the total flow rate is $Q = \sum_{j=1}^n q^j$, we can add the equations above for all layers to obtain

$$Q = \frac{2\pi}{\bar{K}} \sum_{j=1}^n h^j K^j \left(\int_1^{1+L/r_0} \frac{dr}{rk(\sigma^j)} \right)^{-1} \Delta p.$$

We conclude that to maintain the total flow rate constant, we need to impose a time dependent pressure differential:

$$\Delta p = \frac{Q\bar{K}}{2\pi} \left[\sum_{j=1}^n h^j K^j \left(\int_1^{1+L/r_0} \frac{dr}{rk(\sigma^j)} \right)^{-1} \right]^{-1}. \quad (42)$$

This is the adjustment in the pressure boundary layer needed at each time step in a medium consisting of non-communicating layers, each one considered to be homogeneous.

In a medium with n communicating layers, the integrand of equation (38) remains piecewise constant in the z direction and we obtain (42) again to adjust the pressure.

5. NUMERICAL EXPERIMENTS

For the numerical experiments, we consider porosity $\phi = 0.2$, concentration of injected particles $c_i = 10 \text{ ppm}$, $\beta = 250$ and a constant flow rate $Q = 30 \text{ m}^3/\text{day}$. Our mesh is 120×100 and the

computational domain is $[0.1, 0.6] \times [0, 2.5] m$, since we want to know what is happening near the well. We use a time step $\Delta t = 1 \text{ day}$. Our goal is to verify whether there is particle flow between layers and the importance it may have.

Two cases are studied. In the first case, we fix λ and consider a heterogeneous medium, with layers of the same depth, with different absolute permeabilities K_0^j . Then, in the second case we fix K_0 and consider λ^j different in each layer. In each case, we compare the models with and without communication between layers.

5.1. Absolute Permeability

We fix a heterogeneous medium with constant parameter $\beta = 250$ and a filtration function given as $\lambda = 1 - 2\sigma m^{-1}$. The medium has two layers with absolute permeabilities $K_1 = 100 mD$ and $K_2 = 2000 mD$.

To illustrate how particles move in the medium, figure 4 shows the vertical velocity in 10, 100, 200 and 400 days. Notice that there exists a positive velocity, from the less permeable to the more permeable layer and after some time this velocity becomes negative over part of the interface. In this experiment, the maximum vertical velocity is 27.75% of the maximum horizontal one.

Now, we consider the same situation in a six layer medium. In figure 5a, we compare the pressure in a communicating layer model (solid line) and in a non-communicating layer model (dashed line). It is surprising that the difference between them has little significance pressurewise.

5.2. Filtration Function

Let us fix now a six layer heterogeneous medium, with **alternated** absolute permeability $K_1 = K_2 = 100 mD$ and the data from the previous experiment, $\beta = 250$ and $\lambda = 1 - 2\sigma m^{-1}$. Now, we are going to consider that different layers have different filtration functions. In figure 5b, we show the pressure of a non-communicating layers medium (dashed line) and communicating layers (solid line) both with alternating filtration functions $\lambda = 1 - 2\sigma m^{-1}$ and $\lambda = 20(1 - 2\sigma) m^{-1}$.

In this experiment, the maximum vertical velocity is 43.40% of the horizontal one. This is a higher number than in the previous section, (maximum of 27%). It was surprising that despite these higher observed values, communication between layers has little significance pressurewise, as we had seen in figure 5.

A possible answer to the relevance or irrelevance of communication between layers is attempted in figure 6. It shows the concentration of retained particles in our second experiment, with pressure shown in figure 5b. We observe that in fact there is no substantial transport of particles from one layer to another.

6. CONCLUSIONS

We studied two different scenarios for the retention of particles in a layered porous media. Although we observed that the vertical velocity is nontrivial, namely that there is flow between layers, the impact of layer intercommunication was very small for the deposition models

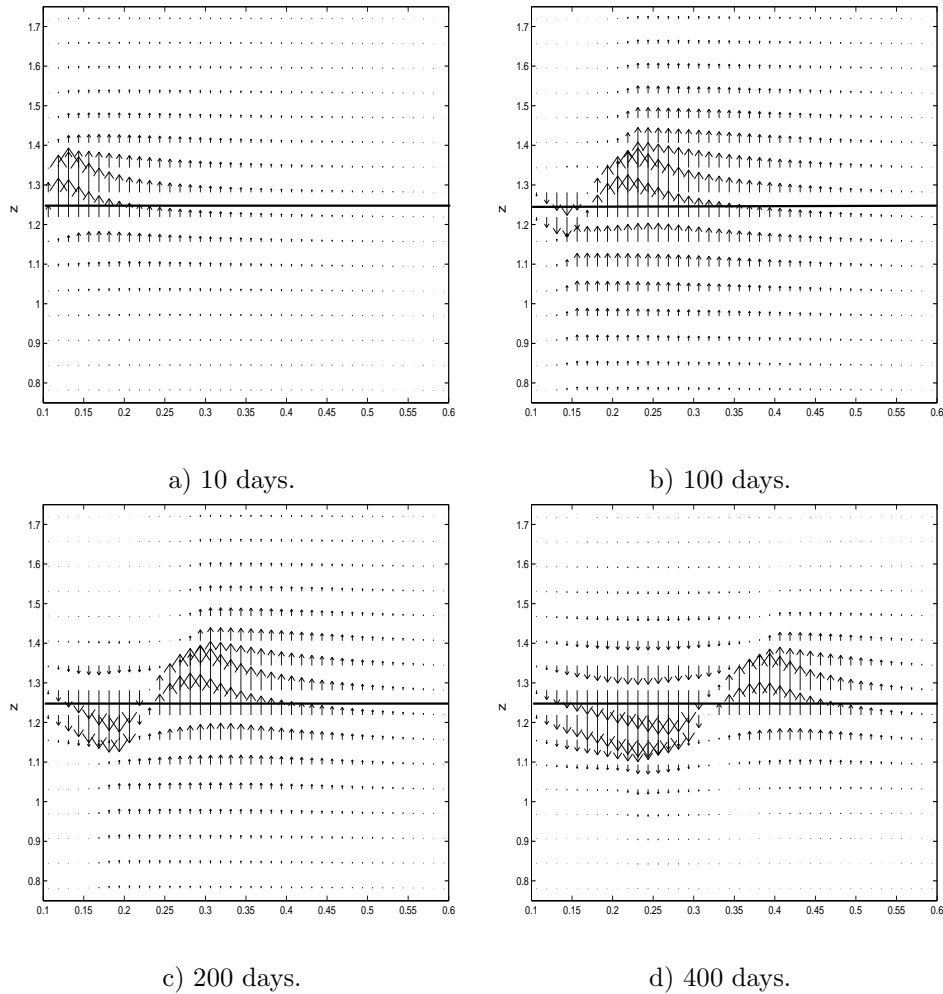


Figure 4. Vertical velocity in distinct absolute permeability layers. The horizontal and vertical axes are r and z . Particle are injected from left to right. The solid line shows the interface between the more permeable layer (top) and the less permeable one (bottom)

considered here. There is a need to study these issues over a broader range of depositon models and parameters.

ACKNOWLEDGEMENTS

This work is part of Julia S. Wrobel's D.Sc. thesis and was supported by the Brazilian Research Council CNPq and by the Brazilian Petroleum Agency, through ANP/PRH 32.

REFERENCES

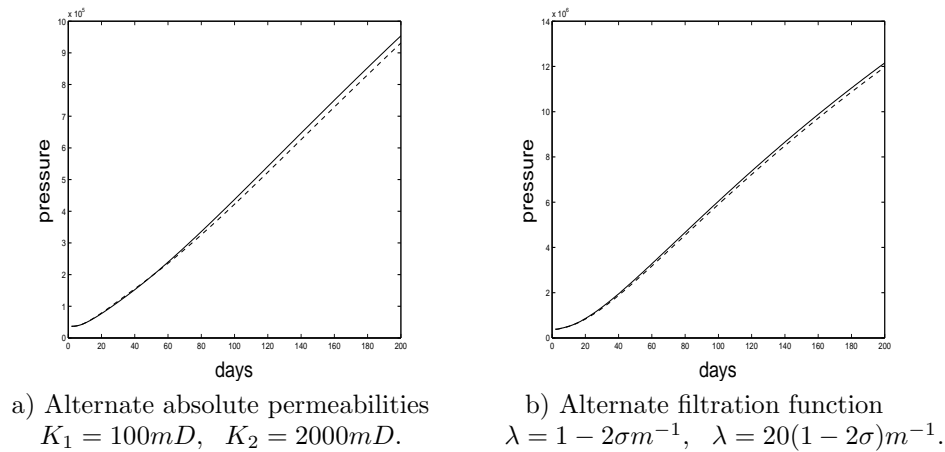


Figure 5. Pressure for communicating layers (solid line) and non communicating layers (dashed line).

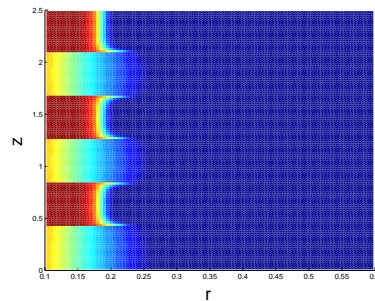


Figure 6. Retained particle concentration in a 6 layers medium with alternate filtration function $\lambda_1 = 1 - 2\sigma m^{-1}$ and $\lambda_2 = 20(1 - 2\sigma)m^{-1}$ after 200 days.

1. A. C. Alvarez. *Inverse Problem for Deep Bed Filtration in Porous Media*. Doctoral thesis, IMPA, 2005.
2. P. Bedrikovetsky, D. Marchesin, F. Shecaira, A. L. Serra, and E. Rezende. Characterization of Deep Bed Filtration System from Laboratory Pressure Drop Measurements. *Journal of Petroleum Science and Engineering*, 32(3):167–177, 2001.
3. P. Bedrikovetsky, D. Marchesin, F. Shecaira, A. L. Souza, and E. Rezende. Injectivity Decline During Injection of Sea/Produced Water. Paper IBP 43300, Proc. Rio Oil and Gas Expo and Conference, Rio de Janeiro, Brasil. 2000.
4. D. Braess. *Finite Elements: Theory, Fast Solvers and Applications in Solid Mechanics*. Cambridge University Press, 1997.
5. J. Douglas, Jr., F. Pereira, and L. M. Yeh. A Locally Conservative Eulerian-Lagrangian Numerical Method and its Application to Nonlinear Transport in Porous Media. *Computational Geosciences*, 4:1–40, 2000.
6. J. Douglas Jr and T. F. Russel. Numerical Methods for Convection-Dominated Diffusion Problems Based on Combining the Method of Characteristics with Finite Element or Finite Difference Procedures. *SIAM J. Numer. Anal.*, 19:871–885, 1982.
7. J. P. Herzig, D. M. Leclerc, and P. Le Goff. Flow of Suspensions Through Porous Media Application to Deep Filtration. *Industrial and Engineering Chemistry*, 62(5):8–35, 1970.
8. S. Pang and M. M. Sharma. A Model for Predicting Injectivity Decline in Water Injection Wells. *SPE 28489*, 1996.
9. P. A. Raviart and J. M. Thomas. *A Mixed Finite Element Method for Second Order Elliptic Problems*. Lecture Notes in Mathematics 606, Springer-Verlag, Berlin and New York, 1977.

10. T. F. Russell and M. Celia. An overview of research on Eulerian-Lagrangian localized adjoint methods, (*ELLAM*). *Advances in Water Resources*, 25:1215–1231, 2002.
11. K. E. Wennberg and M. M Sharma. Determination of the Filtration Coefficient and the Transition Time for Water Injections Wells. *SPE 38181*, 1997.
12. J. S. Wrobel. Perda de Injetividade em Reservatórios Estratificados. Doctoral thesis, IMPA, 2005.